A STUDY OF HYSTERESIS EFFECTS AND TIME RATE OF CHANGE OF REYNOLDS NUMBER IN UNSTEADY FLOW IN TUBES THROUGH THE TRANSITION RANGE

A THESIS

Presented to

the Faculty of the Graduate Division

by

William H. Sims

In Partial Fulfillment

of the Requirements for the Degree

Master of Science in Aeronautical Engineering

Georgia Institute of Technology

June, 1963

In presenting the dissertation as a partial fulfillment of the requirements for an advanced degree from the Georgia Institute of Technology, I agree that the Library of the Institution shall make it available for inspection and circulation in accordance with its regulations governing materials of this type. I agree that permission to copy from, or to publish from, this dissertation may be granted by the professor under whose direction it was written, or, in his absence, by the Dean of the Graduate Division when such copying or publication is solely for scholarly purposes and does not involve potential financial gain. It is understood that any copying from, or publication of, this dissertation which involves potential financial gain will not be allowed without written permission.

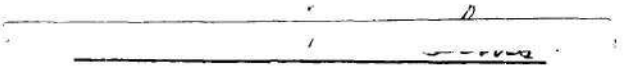

A STUDY OF HYSTERESIS EFFECTS AND TIME RATE OF CHANGE OF REYNOLDS NUMBER IN UNSTEADY FLOW IN TUBES THROUGH THE TRANSITION RANGE

Approved:

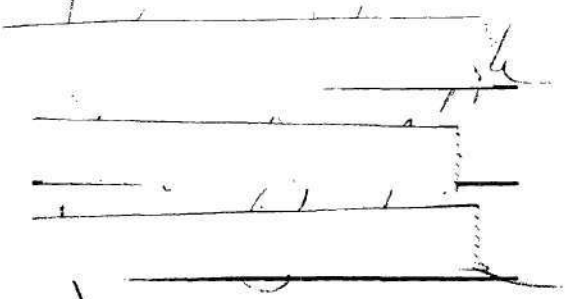

Date Approved by Chairman: Feb 5, 1965

ACKNOWLEDGMENTS

The author wishes to express his deep appreciation to Drs. Arnold L. Ducoffe and Frank M. White, Jr. for suggesting the subject of this thesis, and for their invaluable assistance and patience through all phases of testing and writing. Gratitude is also extended to Dr. K. G. Picha for his critical review of the topic.

A sincere appreciation for the many hours the author was aided by Messrs. George W. Brown and Wilton M. Rooks is gratefully acknowledged, and thanks are expressed to Mr. G. W. D. Cook for his aid in constructing the apparatus.

Thanks are also due the author's wife, Helen, for her patience in typing the manuscript.

Sincere appreciation is extended to the Sandia Corporation for the financial and material aid which made this work possible.

TABLE OF CONTENTS

LIST OF TABLES

LIST OF FIGURES

LIST OF SYMBOLS

A	Cross-sectional area of tube
B	Ratio of metering orifice diameter to entrance pipe diameter
D	Tube inside diameter
E	Thermal expansion correction coefficient
f	Local friction factor, $\tau_w/\frac{1}{2}\rho v^2$
$\bar{f}$	Mean friction factor, $1/L\int_0^L f\,dx$
f^*	Pseudo friction factor, see Eq. I.4
g	Acceleration due to gravity
G	Mass flow per unit area
H_o	Total head pressure
I.D.	Inside diameter
K	Discharge coefficient
L	Tube length
p	Static pressure in tube
P_1	Static pressure upstream of tube entrance
P_2	Static pressure downstream of tube exit
P_I	Static pressure inside upstream end of tube
P_{II}	Static pressure inside downstream end of tube
psid	Pounds per square inch differential
psig	Pounds per square inch gage
R	Gas constant
Rey	Reynolds number

rpm	Revolutions per minute
t	Time, seconds
T	Temperature, degrees Rankine
v	Mean velocity through any cross-section of tube
V	Velocity through metering orifice
w	Rate of mass flow
x	Spatial coordinate
Y	Compressibility factor
ΔP_o	Pressure drop across metering orifice
ΔP_t	Pressure drop across test tube
ρ	Density of air
τ_w	Wall shearing stress
μ	Coefficient of absolute viscosity

SUMMARY

Friction factors in tubes have been the subject of many experimental and theoretical studies in the past. However, the case of unsteady flow through small tubes has remained impregnable to theoretical studies. The purpose of this investigation was to determine the effects of hysteresis and time rate of change of Reynolds number in unsteady flow through small bore tubing through the transition range. Pressure-loss factors for these conditions were obtained by using a steady state analysis, with Reynolds numbers between approximately 400 and 50,000. The pressure-loss factors, which are referred to as pseudo friction factors in this presentation, incorporate the wall friction, development losses, inlet and exit losses, and compressibility effects. The main points of interest in this study were the regimes of transition from laminar to turbulent flow with mass flow increasing, and turbulent to laminar flow, with mass flow decreasing. Hysteresis effects in the transition region were of prime interest also. The unsteady effects were studied, however, for all Reynolds numbers obtained in the laminar and turbulent regions.

The experiments were run at room temperature for a single test tube, using the surge tank total head pressure and the micrometer needle valve rotation speed as the variables. The total head pressure and needle valve speed were varied to give

the range of Reynolds numbers desired for this study.

The theory used for computing the instantaneous pseudo friction factor was based on the assumptions of steady, one-dimensional, continuum flow through constant area tubing, with isothermal changes of state. The test results were compared with the results obtained in an earlier study, with the Hagen-Poiseuille theory for laminar flow in straight tubes, and with the Karman-Nikuradse theory for straight tubes with turbulent flow.

Results of these tests show that there is a hysteresis effect in the transition region, with some effects, also attributable to the unsteady flow, in the laminar and turbulent regimes due to the rate of change of Reynolds number (or mass flow), although the data were too limited for a correlation of the effects.

CHAPTER I

INTRODUCTION

Friction factors in small bore tubes have been the subject of many experimental investigations (1-5)* over the past years. A local friction factor may be defined for small bore tubes as:

$$f = \tau_w / \tfrac{1}{2} \rho v^2 \qquad \text{(I-1)}$$

where f is the local friction factor, τ_w the wall shearing stress, ρ the density of the fluid (air), and v is the mean velocity through the tube.

Both von Kármán (1) and Nikuradse (2) have shown steady flow friction factor data in the regime of turbulent fully-developed flow, while Schlichting (3) has presented data in the laminar fully-developed region as obtained by Hagen (4). At present there is no theory available for determining the friction factor in unsteady flow through small bore tubing.

The solution of the Hagen-Poiseuille (4) equation for steady laminar flow has the form

$$4f = 64/Rey \qquad \text{(I-2)}$$

where Rey is Reynolds number based on tube diameter. The

*Numbers in parentheses refer to the references at the end of the thesis.

semi-empirical equation first obtained by von Kármán and later improved by Nikuradse, valid for fully-developed, turbulent, steady flow, has been shown to be an accurate friction factor relation for smooth tubes, and is given as

$$1/\sqrt{4f} = 2.0 \log_{10}(Re\sqrt{4f}) - 0.8 \qquad (I-3)$$

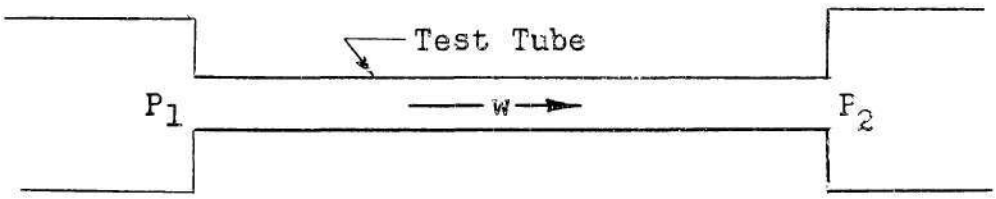

Fig. 1. Equivalent Test System

Lattal (5) used a system as shown in Figure 1 to develop a theory for steady flow using a pseudo friction factor, which he termed $4f^*$. The definition of $4f^*$, as developed in Appendix A, is

$$4f^* = \frac{(P_1^2 - P_2^2)}{RT(\frac{L}{D})G^2} \qquad (I-4)$$

where P_1 is the static pressure upstream of the tube entrance, P_2 is the static pressure downstream of the tube exit, R is the gas constant for air, T is the temperature in degrees Rankine, L/D is the ratio of the tube length to tube inside diameter, and G is the mass flow per unit area.

It should be noted that the pseudo friction factor, $4f^*$, since it is based on P_1 and P_2, includes the wall friction within the tube, compressibility effects, inlet and exit losses and development losses.

The results of Lattal's study were used for a comparison of the pseudo friction factors in the steady state case. The single test tube used throughout the present study was of the same type used by Lattal, although steady state cases were run again in the present study, for verification purposes.

Stone (6) developed a transient theory assuming a quasi-steady, fully developed, compressible, isothermal tube flow, which he used to predict pneumatic pressure lag in simple series systems. Stone's system consisted of a constant area tube attached to a sensing volume. Limited investigations (7) have been conducted with oscillations imposed on a steady flow.

This investigation will be for the purpose of determining the effects, if any, of unsteady flow on the pseudo friction factor as compared with steady state flow for $400 \leq Rey \leq 50,000$, and also to determine whether the time rate of change of the mass flow has any noticeable effect. The effect during both increasing and decreasing mass flow rate has been studied and compared with the results of steady state tests to determine what magnitude of difference in friction factor might be detected that could be attributed to the unsteady flow. The regime of transition will be of interest for obtaining definite knowledge of the form of the friction factor curve in this range of Reynolds numbers. The primary interest in the transition region is the particular manner in which the friction factor varies with Reynolds number, and whether the

variation will remain the same for both increasing and decreasing mass flow rates.

CHAPTER II

APPARATUS

A schematic of the complete apparatus and its components is shown in Figure 2. The pressure source was connected to the system by means of a 3/4-inch copper tube with a pressure regulator inserted between the pressure source and the test system. Flanged, two-inch, steel pipe connected the main components of the system. The pressure taps were placed as shown in Figure 2, and were connected to the differential pressure transducers by means of 1/4-inch copper tubing. All pressure transducers had valves manifolded so as to make it possible to isolate an individual pressure transducer when necessary. A detailed description of the system components follows.

Pressure Source

A 1,000 cubic foot tank (not shown in Figure 2), pressurized to a maximum of 125 psig by means of a 75 horsepower two-cycle compressor, was used as a pressure source. A surge tank, held at a constant pressure for a given test by means of a pressure regulator, was placed between the system and the pressure source.

Valves

The flow rates were controlled by a micrometer needle valve

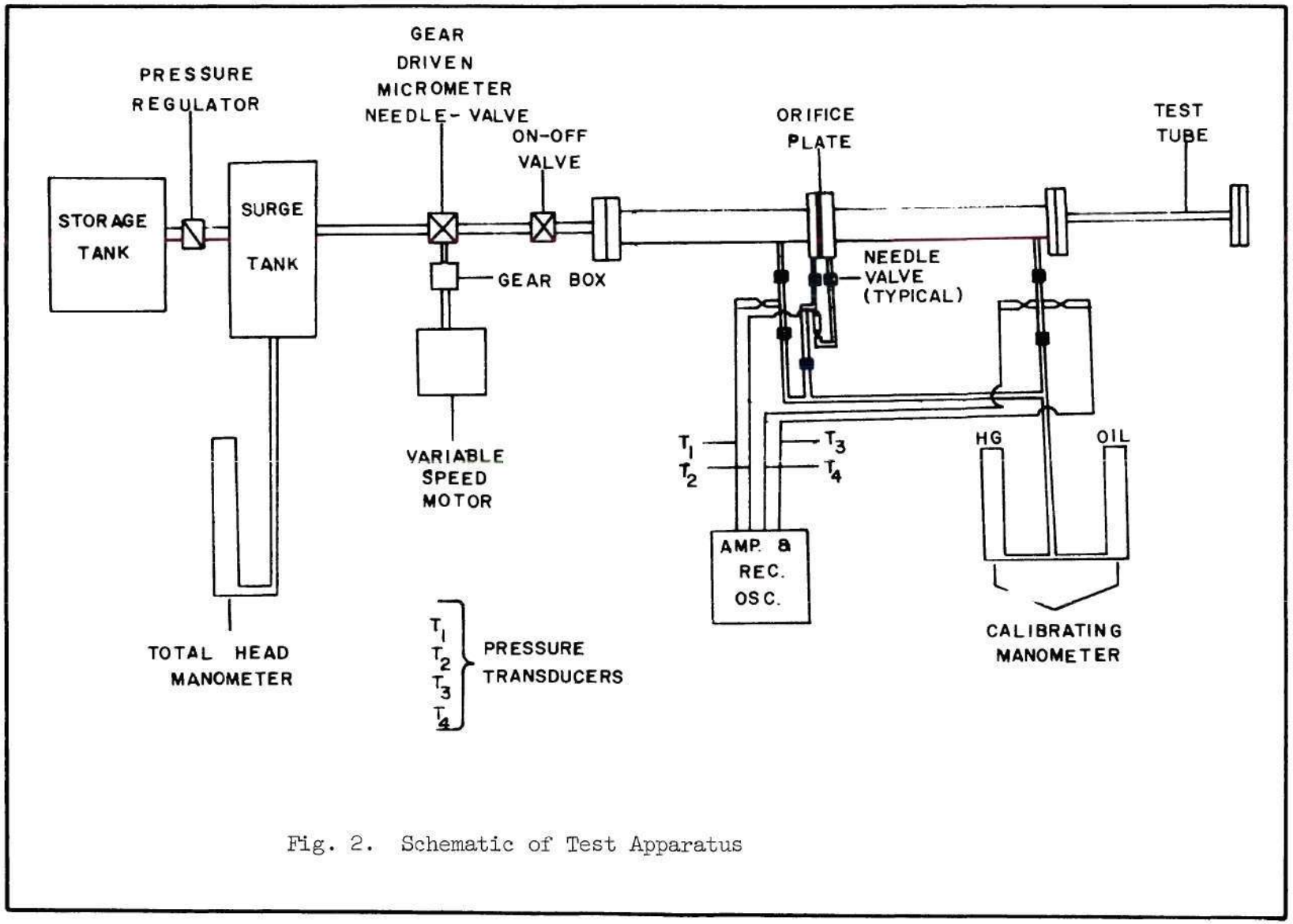

Fig. 2. Schematic of Test Apparatus

having twenty revolutions from the full-closed to the full-open positions. The micrometer needle valve was mechanically driven by a variable speed motor and gear train. A rubber diaphragm shut-off valve was placed upstream of the entrance to the system for safety purposes and for easier checking for leaks. A blank flange plate was incorporated on the downstream end of the system to enable checking for leaks.

Metering Orifice

Flow rates were determined (see Appendix B) using an ASME (8) standard, sharp-edged, metering orifice having a B ratio of 0.1, where B is the ratio of the metering orifice diameter to the entrance pipe diameter (D_2/D_1). Flange taps were employed to determine the pressure drop across the orifice plate, which was constructed from stainless steel.

The mass flow was determined by the ASME steady flow theory due to the lack of a method of measuring an unsteady mass flow.

Pressure Measurements

Electrically activated differential pressure transducers were used to measure all pressures. For static pressures one side of the transducers was open to the atmosphere for reference. The pressure drop across the orifice plate was measured in the conventional manner, i.e., one pressure tap to each side of the transducer. All transducers were readily accessible,

and when increased range of pressures was indicated, the transducers could be replaced by one of higher differential pressure rating. Table 1 lists the range of the transducers used throughout the tests, while Table 2 gives the differential pressures experienced by the respective transducers. It was necessary in some cases to use as many as three transducers simultaneously for measuring the pressure drop across the orifice and the static pressure upstream of the test tube. A single transducer was used for measuring the static pressure upstream of the orifice. The pressure measured at this point was referenced to atmospheric pressure before being used in any calculations, thereby making it unnecessary to have the extreme sensitivity required at the other two points. The use of two or three transducers at other stations was necessary in order to increase the sensitivity at low mass flow rates while having a large range of pressure variations possible. When the more sensitive transducer reached its maximum deflection on the record trace, it was manually isolated from the system by cut-off valves placed on either side of each transducer in order to completely isolate the transducer from either the calibrating system or the test system. These valves are shown in Figure 3.

Gears and Drives

A reversible, variable speed motor with a 6:1 range was used to drive a 20:1 reduction gear system. The input speed

Table 1. Pressure Transducers

Total Head, psig	Transducer Ratings, psid						
	T_1	T_2	T_3	T_4	T_5	T_6	T_7
100	15.0	0.1	2.0	7.5	0.15	2.0	10.0
60	15.0	0.1	2.0	7.5	0.15	2.0	10.0
40	7.5	0.1	2.0	2.0	0.15	2.0	5.0
20	5.0	0.1	*	2.0	0.15	*	2.0
10	2.0	0.1	*	1.0	0.15	*	2.0
5	2.0	0.1	*	0.5	0.15	*	1.0

* Transducer not used

T_1 Static pressure upstream of orifice

T_2 Pressure difference across orifice, low range

T_3 Pressure difference across orifice, medium range

T_4 Pressure difference across orifice, high range

T_5 Static pressure upstream of test tube, low range

T_6 Static pressure upstream of test tube, medium range

T_7 Static pressure upstream of test tube, high range

Table 2. Transducer Pressure Ranges

Total Head, psig	T_1	T_2	T_3	T_4	T_5	T_6	T_7
100	14.8	0.03	1.15	5.50	0.05	1.80	9.70
60	9.0	0.03	1.15	3.50	0.05	1.90	5.40
40	6.0	0.03	1.15	2.00	0.05	2.00	3.70
20	4.0	0.03	*	1.50	0.05	*	2.00
10	2.0	0.03	*	0.85	0.05	*	1.50
5	1.3	0.03	*	0.50	0.05	*	1.10

* Transducer not used

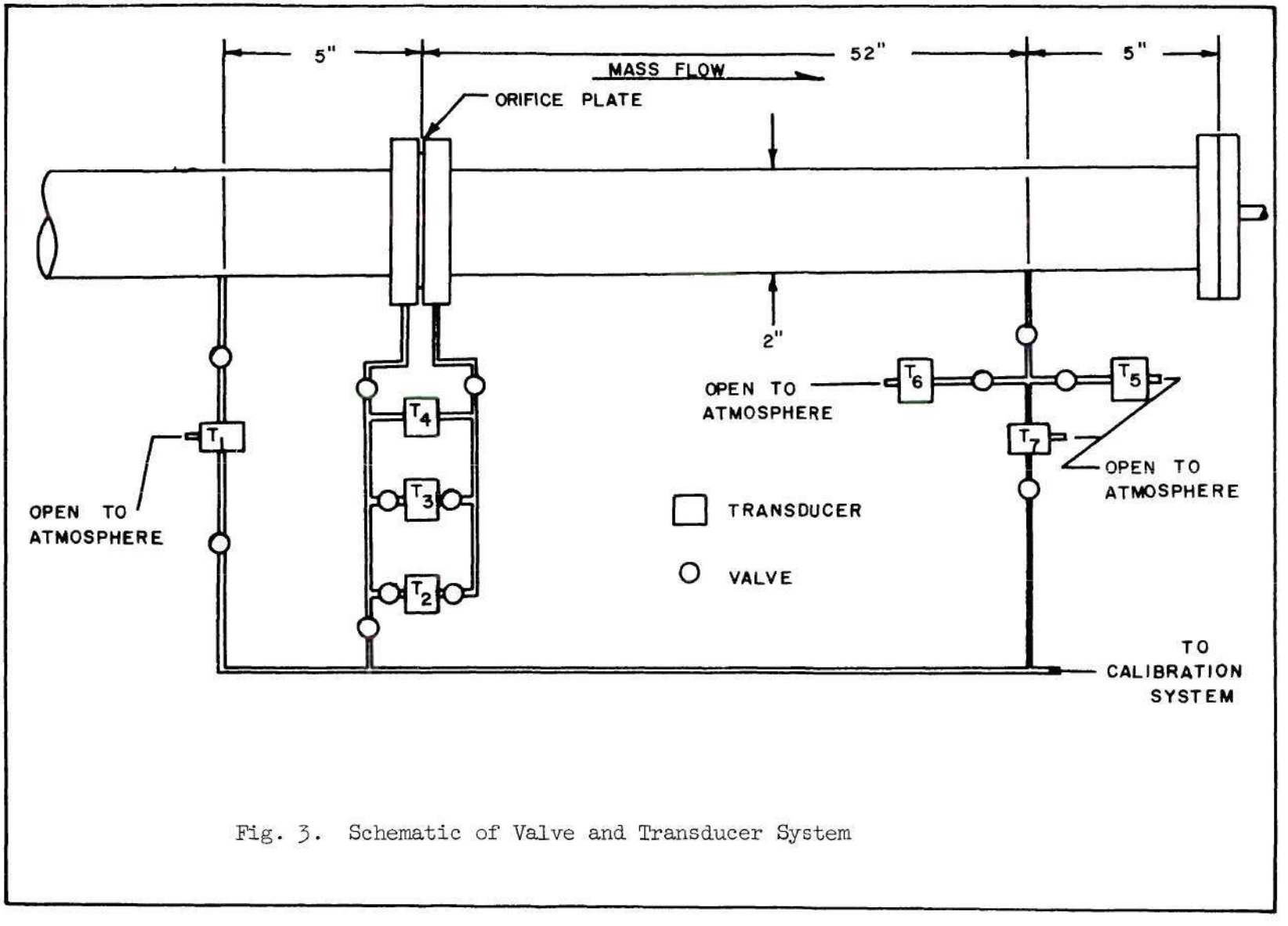

Fig. 3. Schematic of Valve and Transducer System

of the motor was 1750 rpm, with output speeds of 450 rpm maximum and 75 rpm minimum. The drive speed to the micrometer needle valve was variable between 3.75 rpm to 22.5 rpm. For test purposes the drive shaft was operated at 4 and 20 rpm.

The motor and gear system was mounted on a "saddle" that enabled isolation of the micrometer needle valve system from the test apparatus. This was necessary in order to keep the vibrations in the test apparatus to a minimum.

Test Tubing

The tube tested was a commercially bought seamless steel tube. The tube inside diameter was 0.290 inches, and was 145 inches long. The test tube was integrated into the system with a 37-degree flare fitting on each end.

Power Supplies and Recording Equipment

The electronic recording equipment consisted of an oscillator-power supply combination, seven separate amplifiers, and a recording oscillograph.

The oscillator-power supply provided the filament voltage, the regulated plate voltage, and a three kilocycle carrier frequency for the amplifiers. The power supply also provided the excitation voltage for the differential pressure transducers.

The output signals from the seven pressure transducers were fed into separate amplifiers. The basic components of

each amplifier were the balancing portion of the transducer bridge network, an attenuator, a three kilocycle carrier amplifier, and a demodulator.

CHAPTER III

PROCEDURE

Prior to each test the differential pressure transducers were calibrated with either an oil or mercury micro-manometer, depending on the transducer pressure range. The more sensitive transducers (±0.1 and ±0.15 psid) were calibrated with an oil micro-manometer, and the less sensitive (±1.0 psid or greater) with a mercury micro-manometer. After completion of the calibration the 1,000 cubic foot storage tank was pressurized to a maximum of 125 psig. The test system was then pressurized to approximately 15 psig to check for leaks, with all transducers being isolated from the system during this procedure. The total head pressure in the surge tank was then regulated to the value required for the tests to be conducted. A detailed description of the test procedure, using the test with a total head pressure of 60 psig as a reference, is described below.

Test Run

With the rubber diaphragm safety valve closed a zero reference trace was taken on the recording oscillograph. After the safety valve was opened, the recorder was started, and the variable speed motor, set for a drive speed of 4 rpm, was turned on. As the micrometer needle valve was opened at a constant rate, the mass flow increased. The very sensitive

transducers, T_2 and T_5, reached their maximum deflection on the record trace approximately ten seconds after the motor was started. The cut-off valves to these transducers were closed at this point. The number of revolutions the needle valve had opened was noted here in order to have a reference point for re-opening the valves during the decreasing mass flow portion of the test. The medium range transducers, T_3 and T_6, reached their maximum deflection approximately 35 seconds later, and were isolated from the system by means of their cot-off valves. Again the number of revolutions the micrometer needle valve had made was noted for later reference.

The mass flow was allowed to continue to increase until the maximum deflection of the high range transducers, T_4 and T_7, was reached. At this point the variable speed motor was turned off, and steady state flow allowed to develop.

To begin the decreasing mass flow portion of the test, the drive motor was reversed and turned on. When the mass flow had decreased to the proper limit, the medium and low range transducers were again subjected to the flow by opening the valves that had been closed during the increasing mass flow test.

Upon completion of the test run the rubber diaphragm safety valve was again closed and another reference record made on the trace.

A total of four tests were run for each surge tank pressure, two each at both minimum and maximum needle valve

speeds. This was done in order to check on repeatability.

After all four tests were completed, a second calibration was made to check on the initial calibration.

Reduction of Data

The method by which the experimental data was reduced may be explained in the following qualitative manner. The use of multiple transducers at the orifice plate and entrance to the test tube allowed an overlap of pressure readings in the data. In the data reduction scheme, the pressure reading of a less sensitive transducer was matched with the pressure reading of the more sensitive instrument in order to insure continuity in the readings. In the process of reducing the data to a working form, it was seen that, even though the pressure readings were referenced to the more sensitive instruments for the increasing mass flow case, the decreasing mass flow evidenced properties that required that the data be analyzed as if it were always increasing mass flow. This procedure allowed the less sensitive always to be referenced to the more sensitive transducers for an increasing pressure level flow.

Accuracy

The accuracy of the calibrations and the errors in reading the oscillograph records comprise the greater part of the error in the data. The calibrations taken before and after each test run were used for reduction of the data for each test. Errors produced by non-linearity of the amplifier-trans-

ducer circuit were of the order of ±2.5% of full scale in the calibrations of the transducers. The reduction of the data from the oscillograph records resulted in maximum errors of ±½% of full scale. It should be borne in mind, however, that as these errors might be introduced into the calculation of $4f^*$ by Equation (A-9), the magnitudes of the total error by both accumulation and the fact that the static pressures and the mass flow terms are squared, could result in as much as 10% total error. However, since such unfortuitous circumstances would be extremely rare, the total errors are necessarily of a lesser magnitude than this conservative figure.

CHAPTER IV

DISCUSSION OF RESULTS

The general results of these tests will be compared with the theoretically predicted and experimentally determined values of $4f^*$, for steady flow, of Karman-Nikuradse, Hagen-Poiseuille, and Lattal. The results will necessarily be confined to the single test tube. The tube was 145 inches long, with a 0.290 inch inside diameter (L/D=500). All tests were conducted at room temperature, varying from 540-550 degrees Rankine.

Figure 4 represents the results of the steady state tests run for comparison purposes. When compared with the classical Hagen-Poiseuille and Karman-Nikuradse curves it may be seen that the present results are typically larger for a given Reynolds number except for very small Reynolds numbers. This is due to the losses included in the present results that are not included in the classical theories. It may be seen that transition occurs for a lower Reynolds number (that is, the unsteady flow diverges from the laminar steady state data), which is attributable to the rate effects.

Figure 5 relates the time history of the mass flow, in terms of the Reynolds number, for the total head pressures used in the present tests. The maximum Reynolds numbers, and thus mass flows, may be seen to be the same magnitude for both

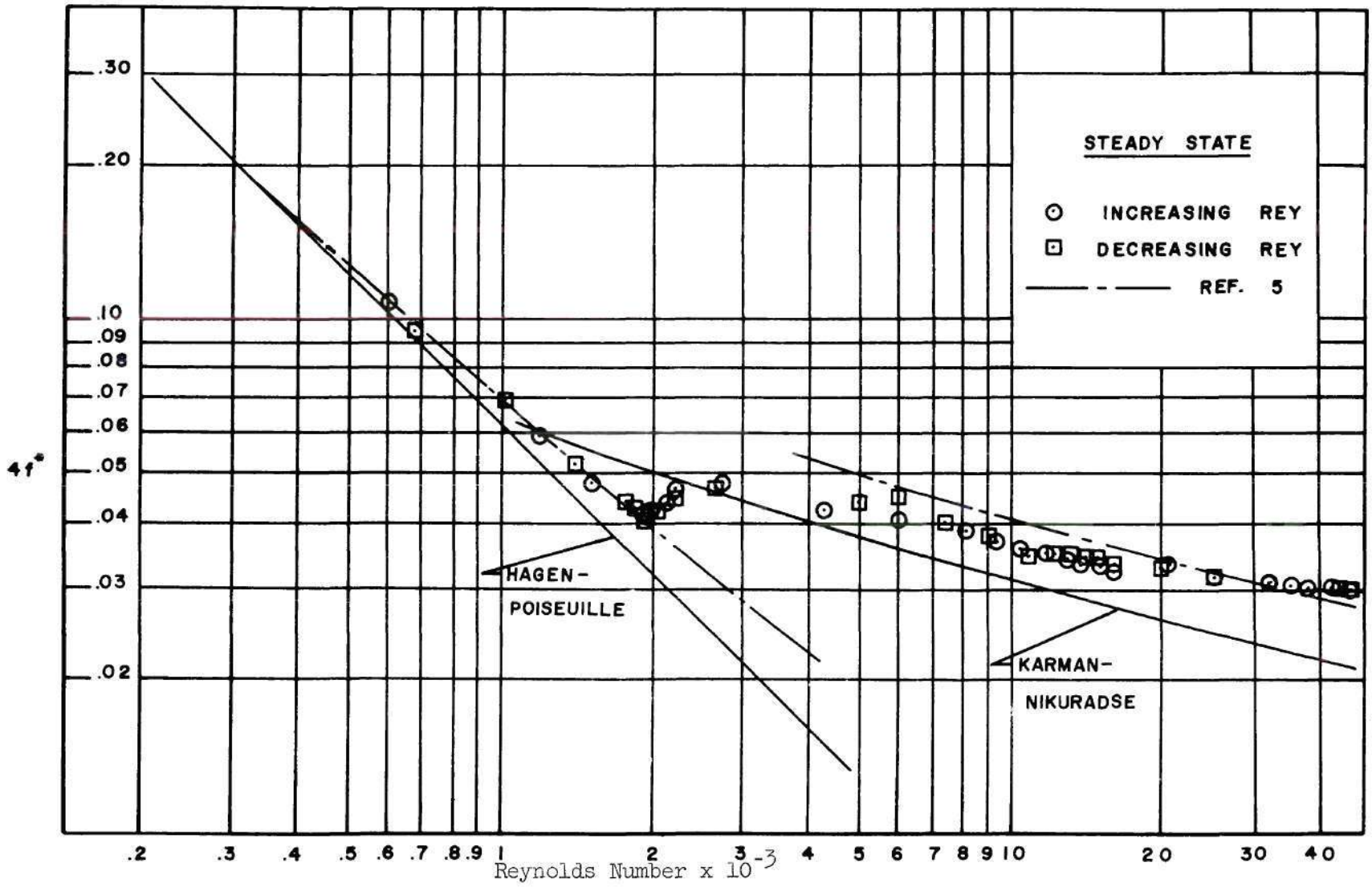

Fig. 4 Steady State Pseudo Friction Factor as a Function of Reynolds Number

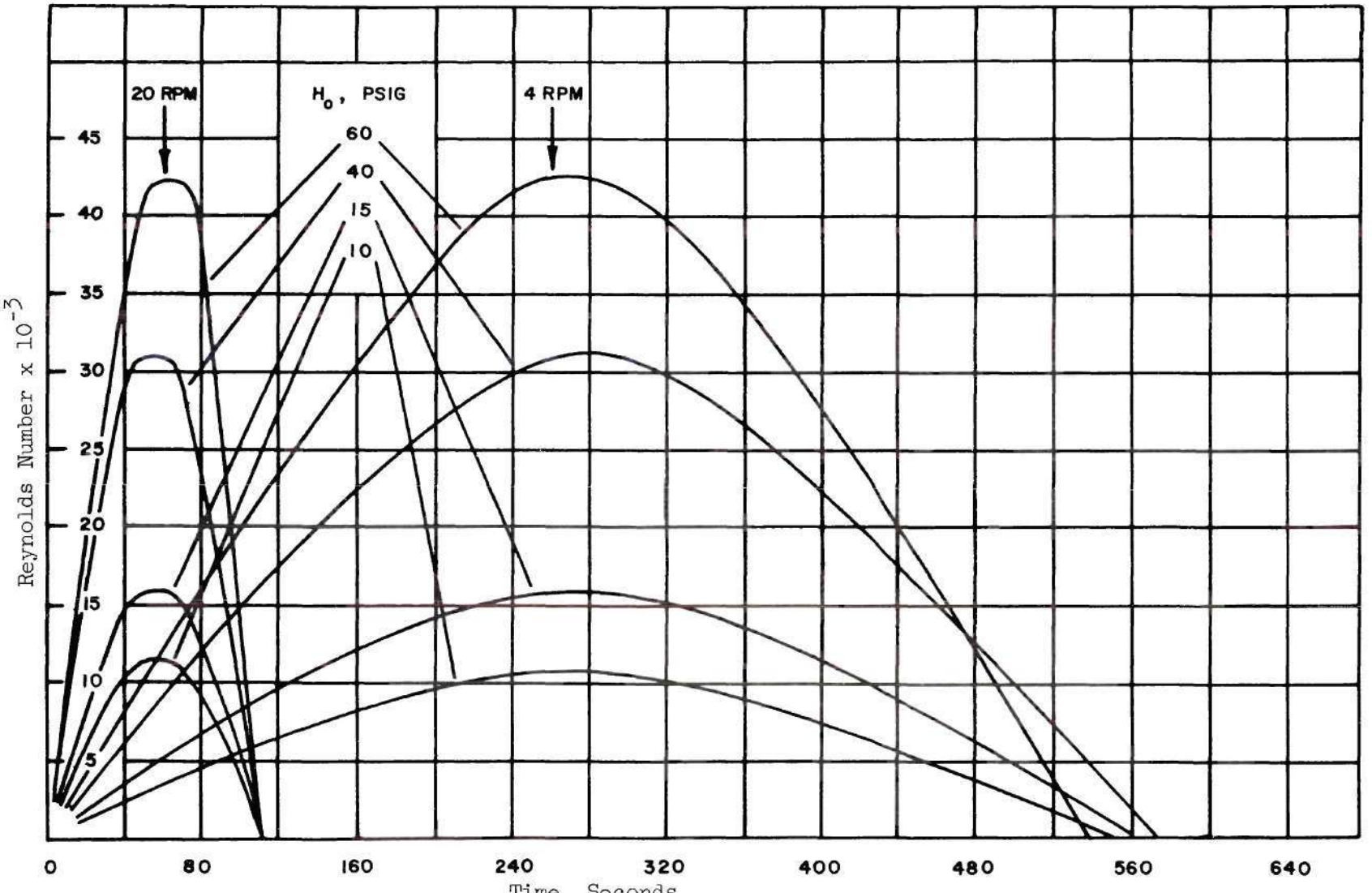

Fig. 5 Time History of Reynolds Number

the fast and moderate needle valve rates for a typical total head pressure. The curves showing a time lapse of approximately 110 seconds is for the fast needle valve rate (20 rpm), while the 560 second values correspond to the slow valve speed of 4 rpm.

A typical run, illustrated in Figure 6, shows the pseudo friction factor as a function of Reynolds number. This particular result is for a total head pressure of 40 psig and a run time of approximately 560 seconds. For this test, the micrometer needle valve was driven at a speed of 4 rpm. For comparison purposes, the steady state curves are also shown. Several observations may be made from the data of Figure 6.

First, in the laminar region, the results compare very favorably with the steady state values for both increasing and decreasing Reynolds numbers, although the values of the pseudo friction factor are slightly higher for decreasing mass flow. In the turbulent region, with practically negligible scatter evidenced, the values of $4f^*$ are typically those of steady state flow. The agreement of the unsteady experimental results with those of steady state tests is indeed gratifying.

The transition region is clearly defined by the smooth variation in $4f^*$, although this phase does encompass a change in Reynolds number of approximately 1200. The transition region may be seen as developing at a Reynolds number as low as 1800 and extending to a value of approximately 3500-4000.

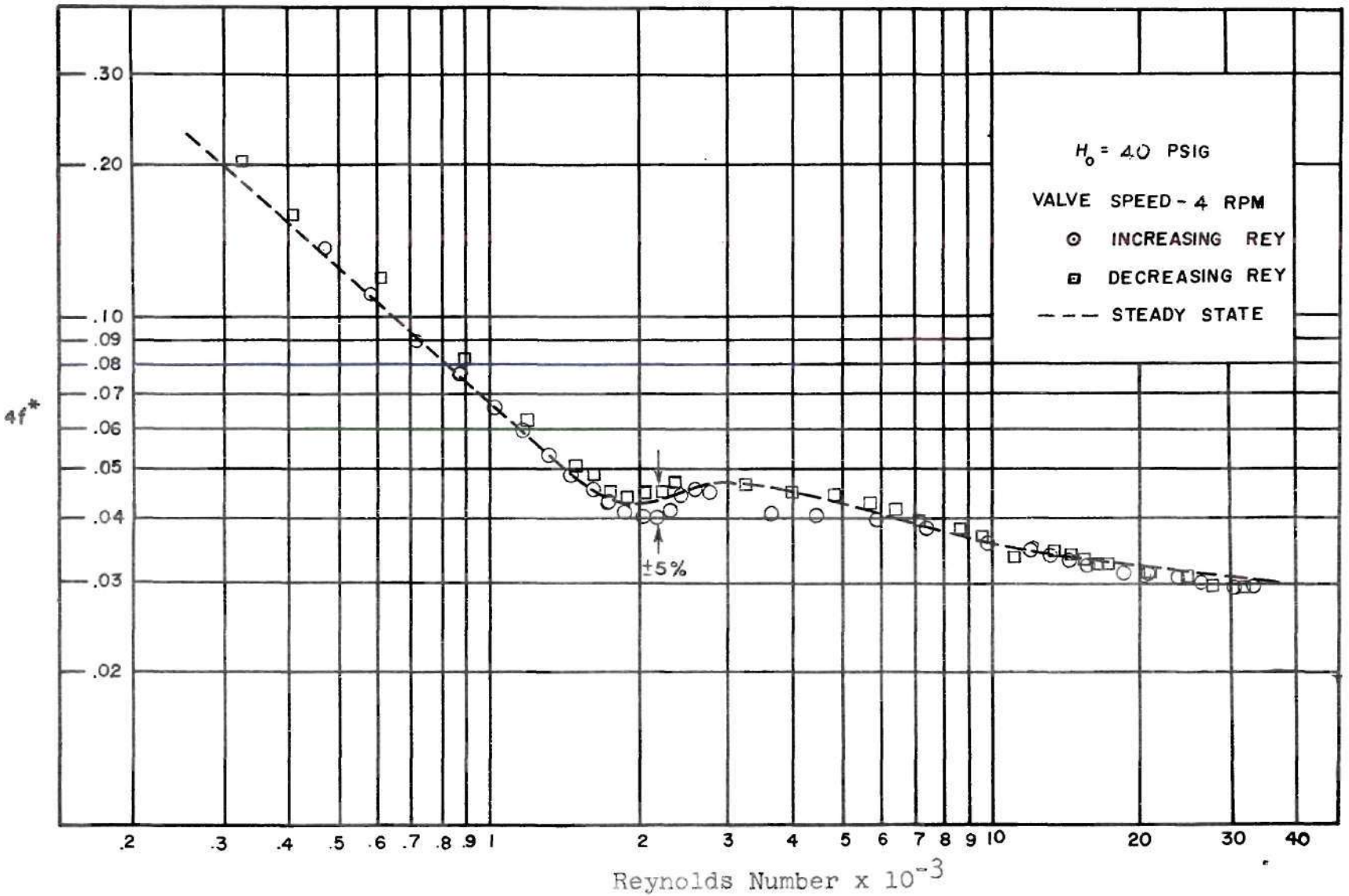

Fig. 6 Pseudo Friction Factor as a Function of Reynolds Number

Shown in Figure 7 is the corresponding test run for a needle valve rate of 20 rpm and a total head pressure of 40 psig. There is more evidence of scatter in the laminar region for this test than the slow rate test. The scatter of test points in the laminar region is due to the hysteresis effects induced into the system by the increased rate of change of mass flow.

The reason for the higher values of pseudo friction factor in the transition region for decreasing mass flow was the hysteresis in the system. The character of the $4f^*$ versus Reynolds number curve is necessarily changed by the hysteresis effects, which are basically reflections of the rate of change of Reynolds number. It is to be expected that since mass flow rate effects are large they would be more pronounced in this region.

Shown in Figures 8 and 9 are plots of the pressure drop across the test tube, ΔP_T, as a function of the pressure drop across the orifice plate, ΔP_o. Figure 8 shows a typical variation of ΔP_T versus ΔP_o for a moderate needle valve opening rate. The agreement between increasing and decreasing mass flow rates may be seen to be very good, as was true for all the tests.

Figure 9 shows the agreement of pressure drops for several test runs, and here it should be pointed out that any rate effects in pressure drop that are present are apparently negligible, since the curves for the moderate and fast needle

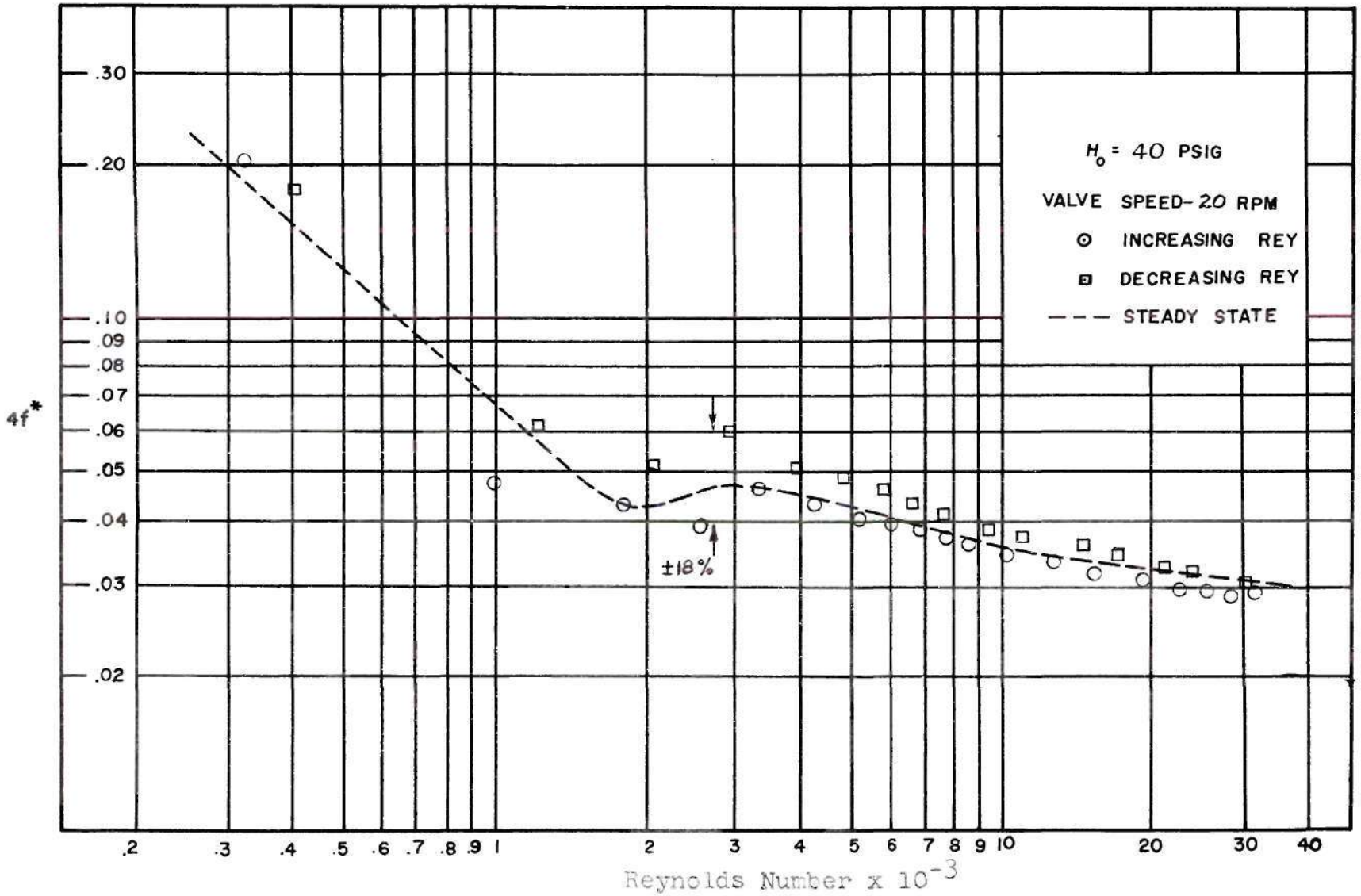

Fig. 7 Pseudo Friction Factor as a Function of Reynolds Number

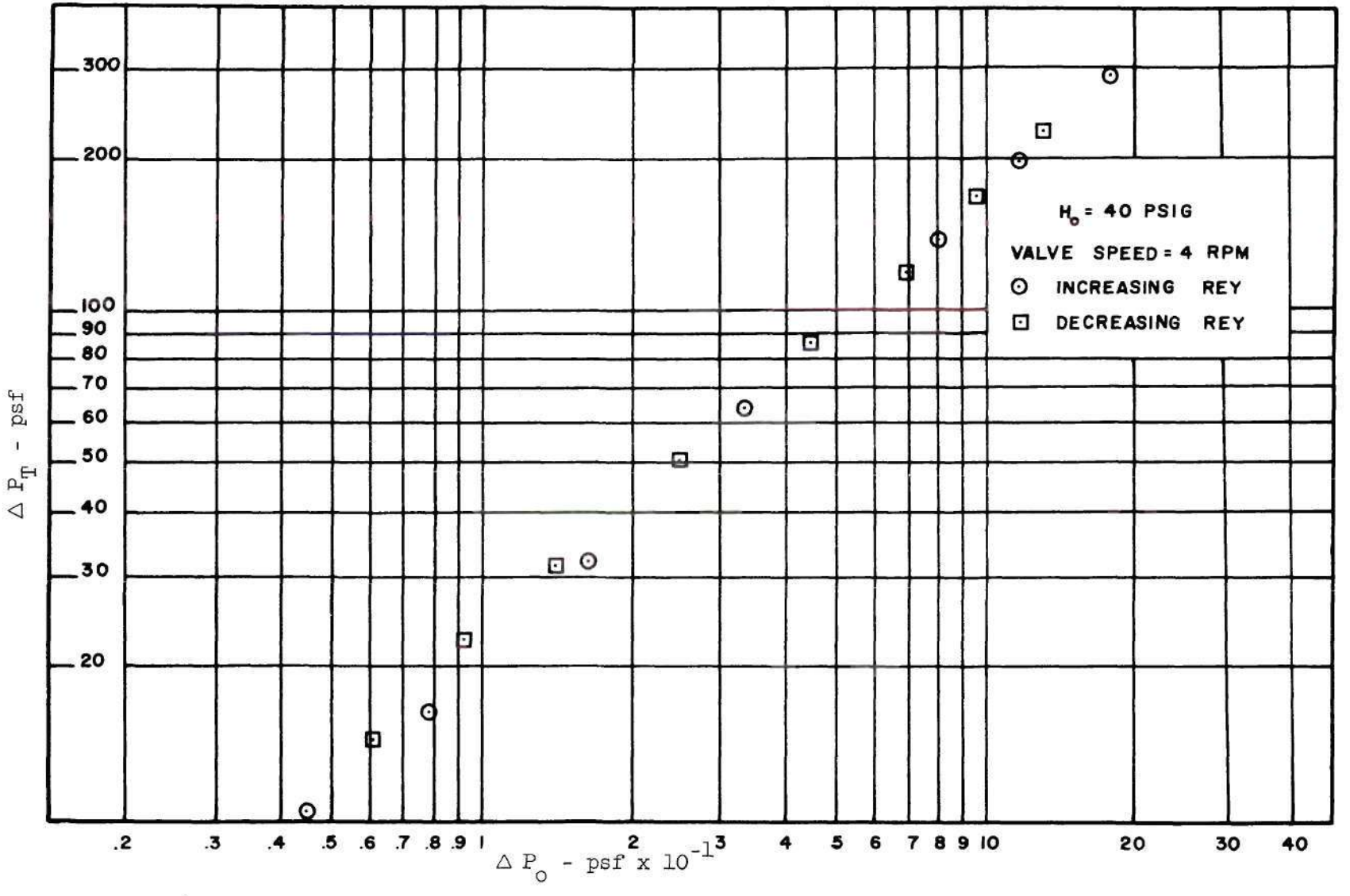

Fig. 8. Pressure Drop Across Test Tube as a Function of Pressure Drop Across Orifice

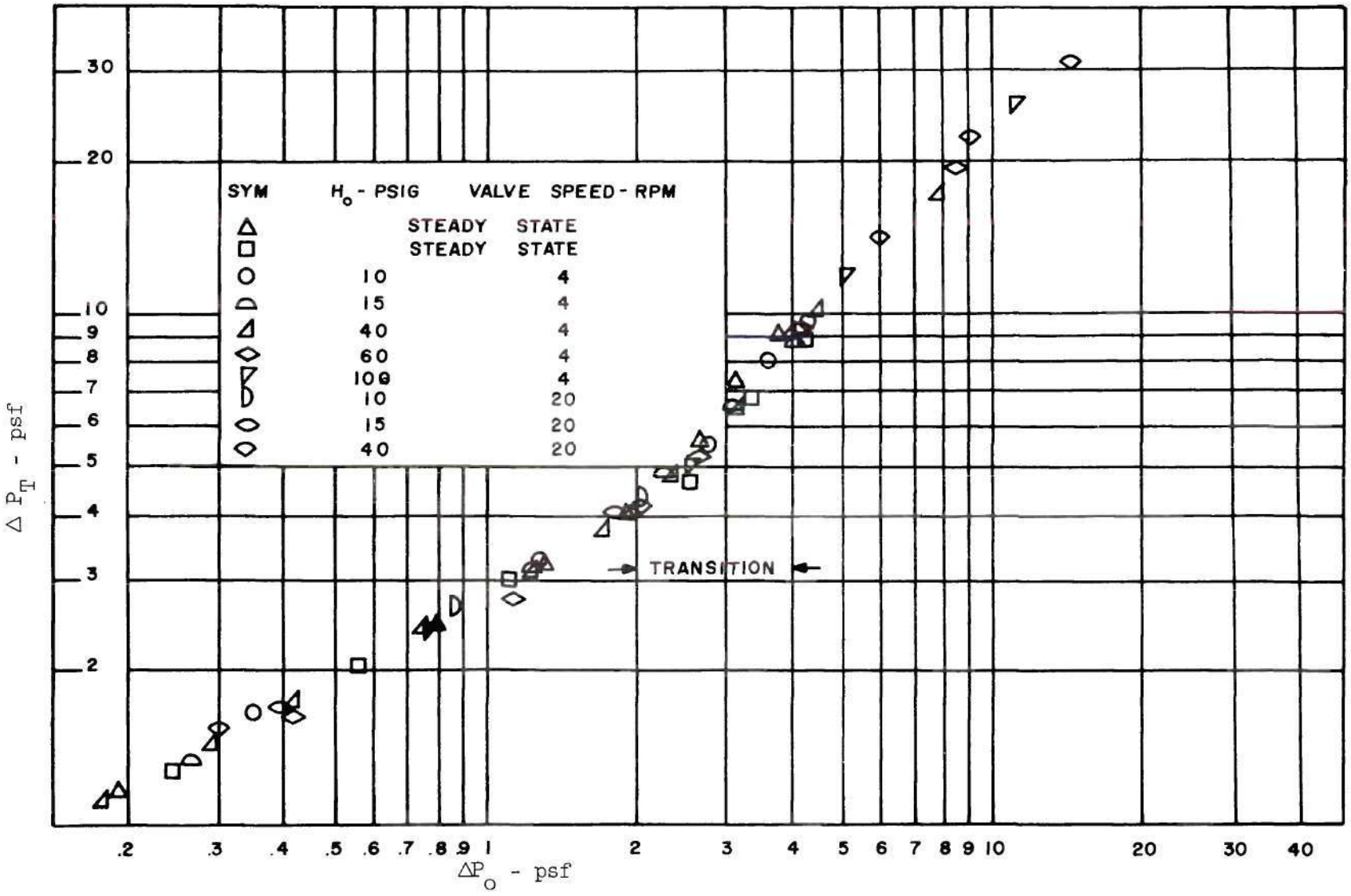

Fig. 9. Pressure Drop Across Test Tube as a Function of Pressure Drop Across Orifice

valve opening rates are inseparable in these illustrations. Included in Figure 9 is the steady state values as obtained in the present tests, and which agree with those results obtained by Lattal. The correlation shown in Figure 9 appears to indicate that instantaneous mass flow rates may be predicted for unsteady flows by instantaneous pressure drops across an orifice plate.

Figures 10-15 show further results of the present tests. The effects and comparisons are, in general, typical of those compared earlier in the text.

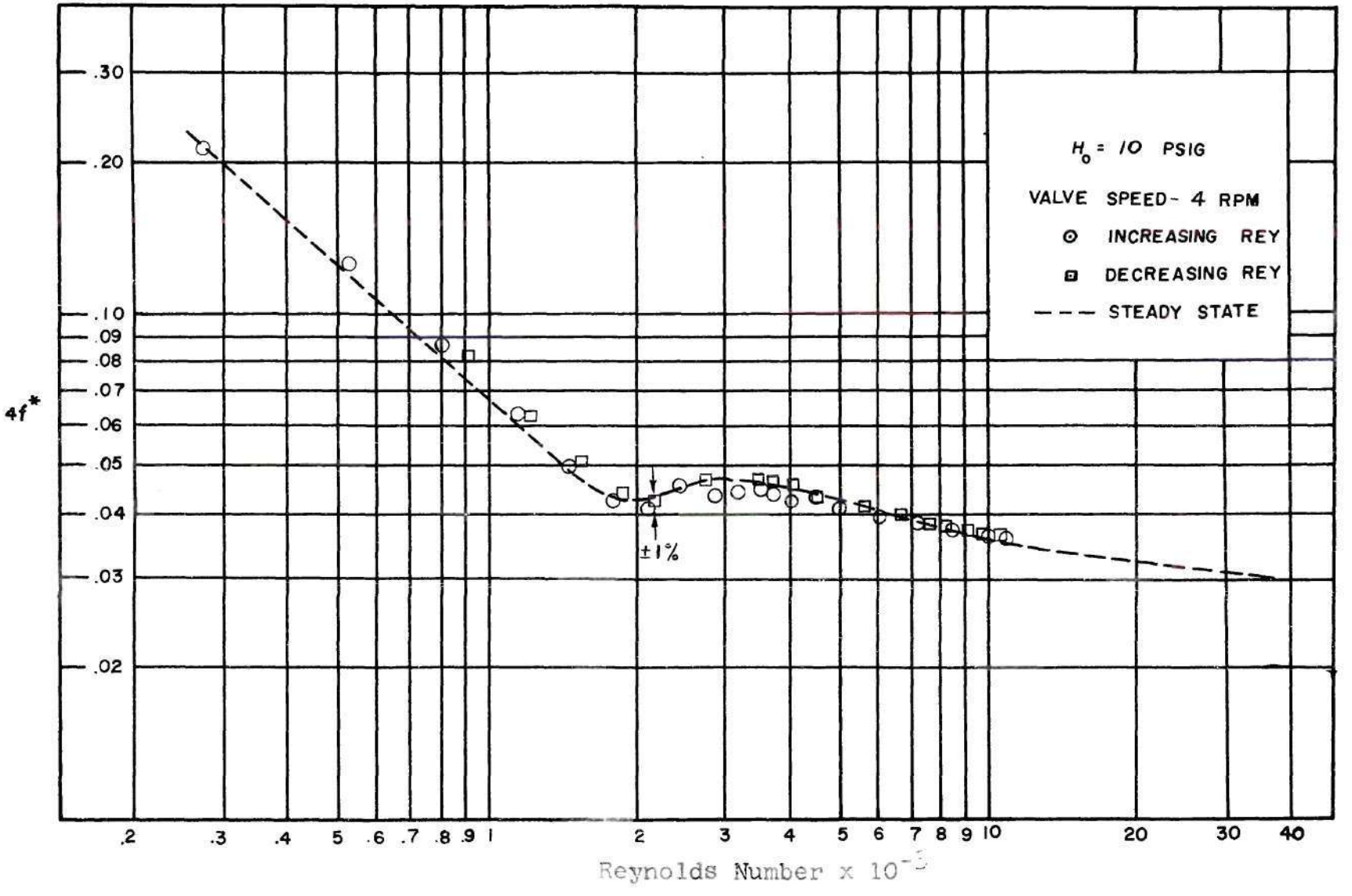

Fig. 10 Pseudo Friction Factor as a Function of Reynolds Number

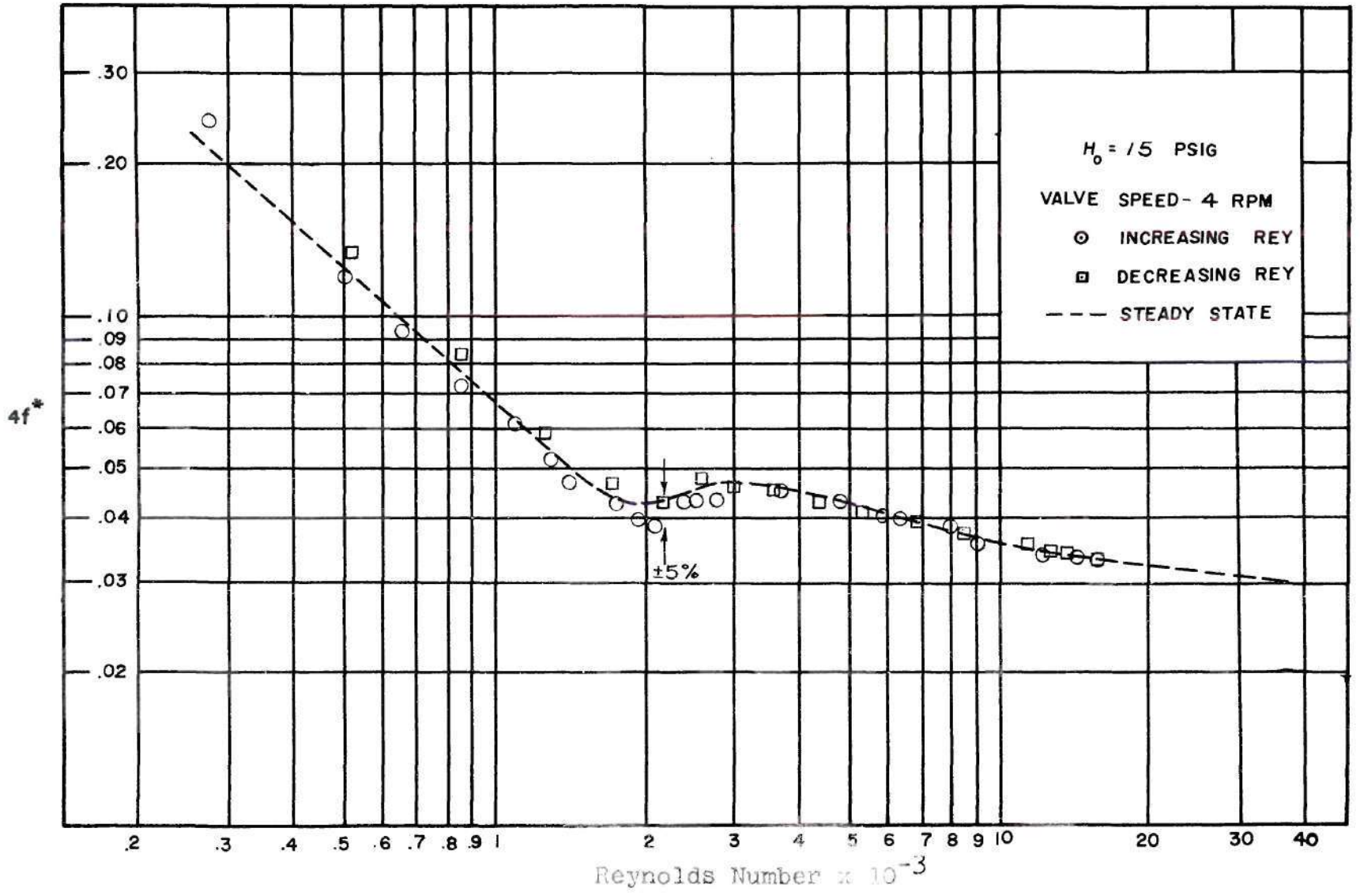

Fig. 11 Pseudo Friction Factor as a Function of Reynolds Number

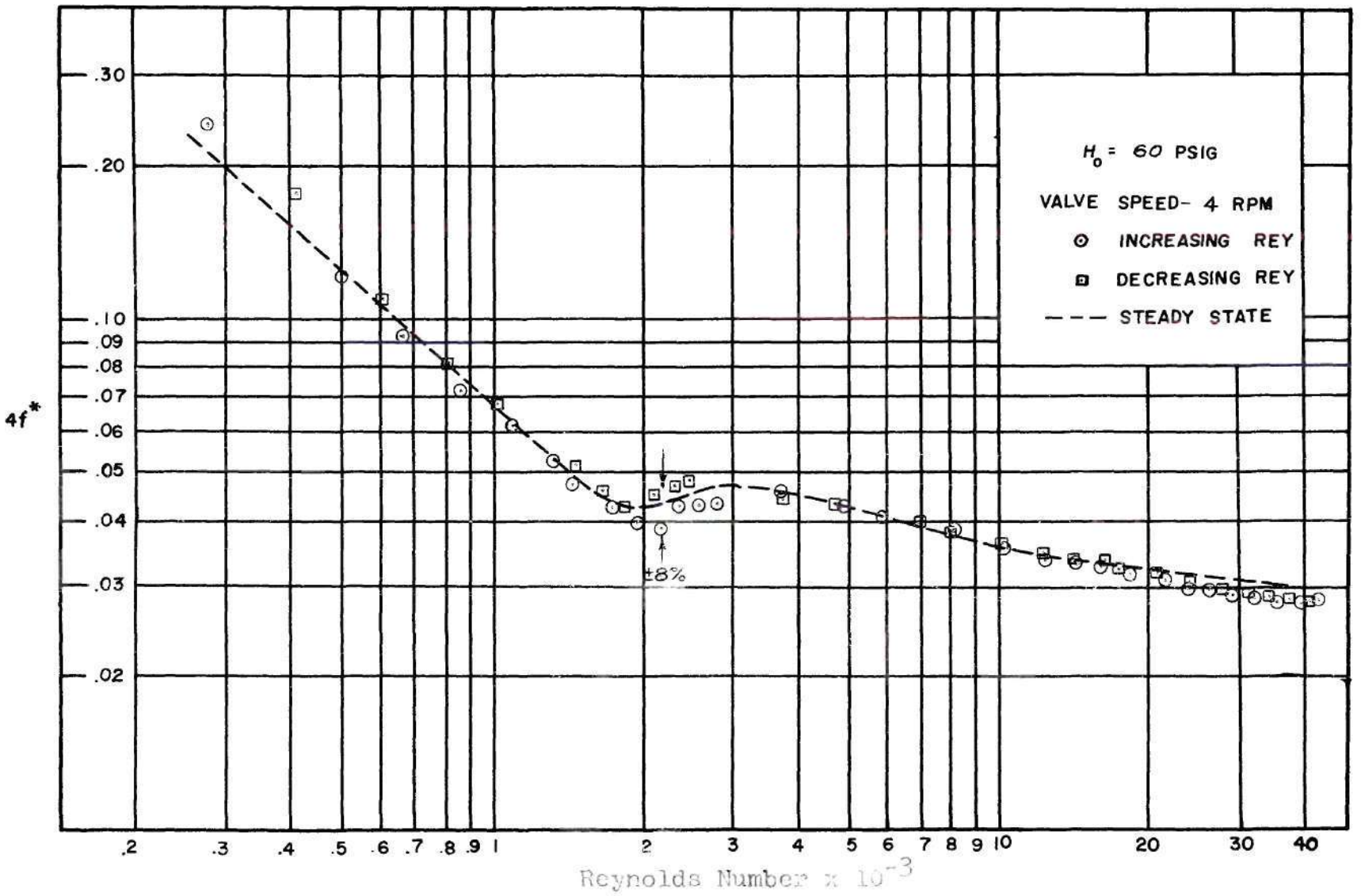

Fig. 12 Pseudo Friction Factor as a function of Reynolds Number

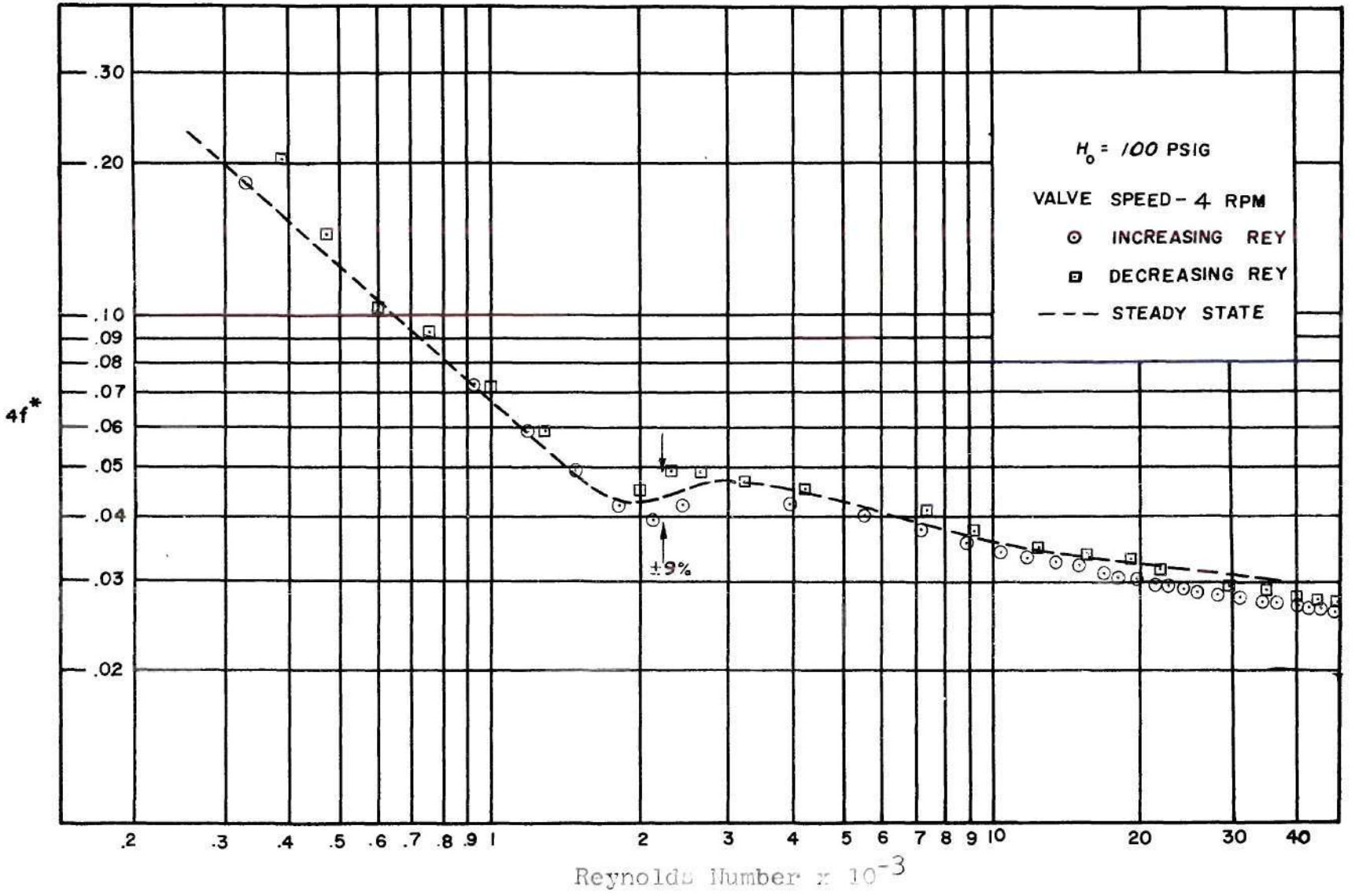

Fig. 13 Pseudo Friction Factor as a Function of Reynolds Number

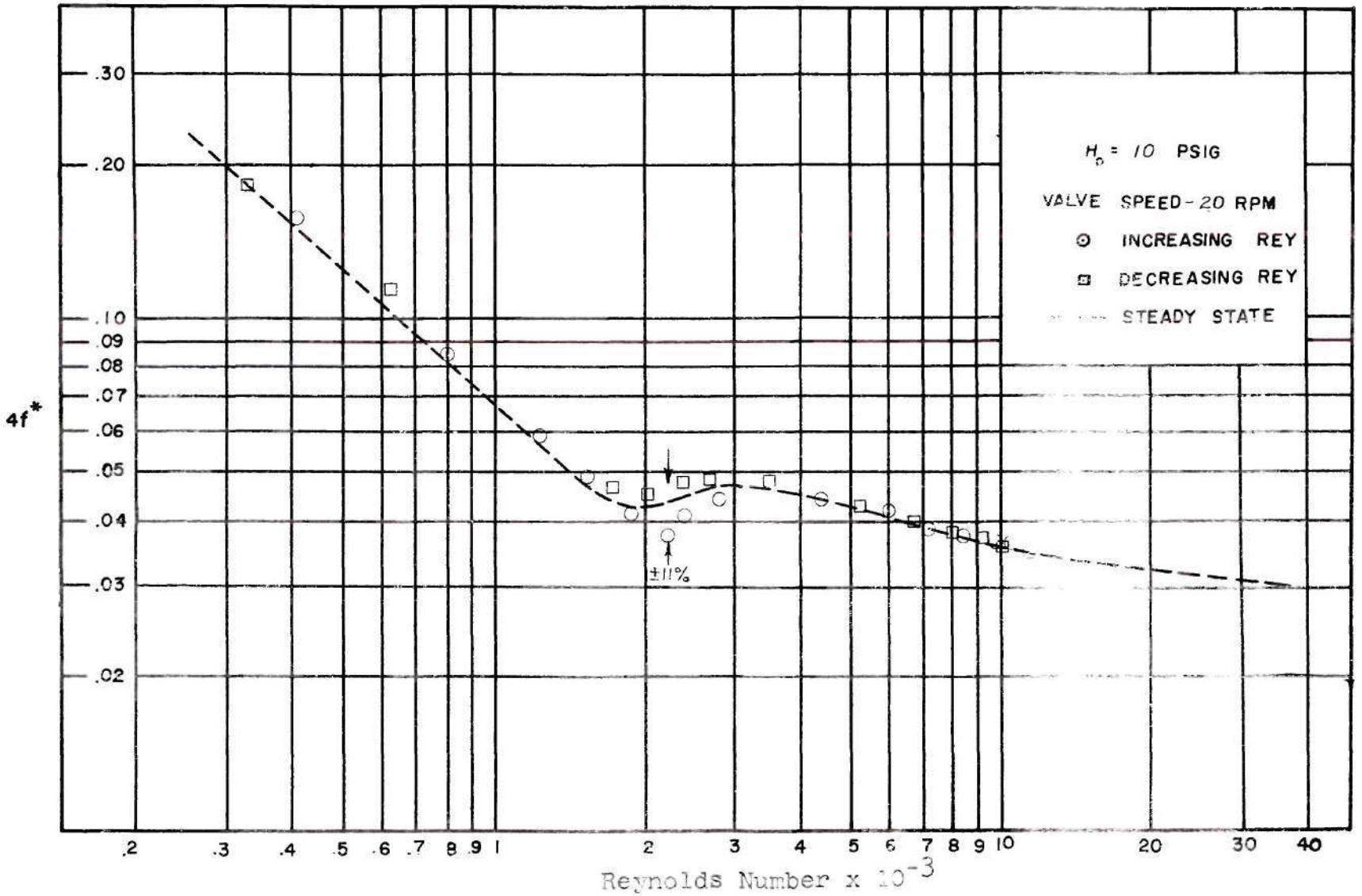

Fig. 14 Pseudo Friction Factor as a Function of Reynolds Number

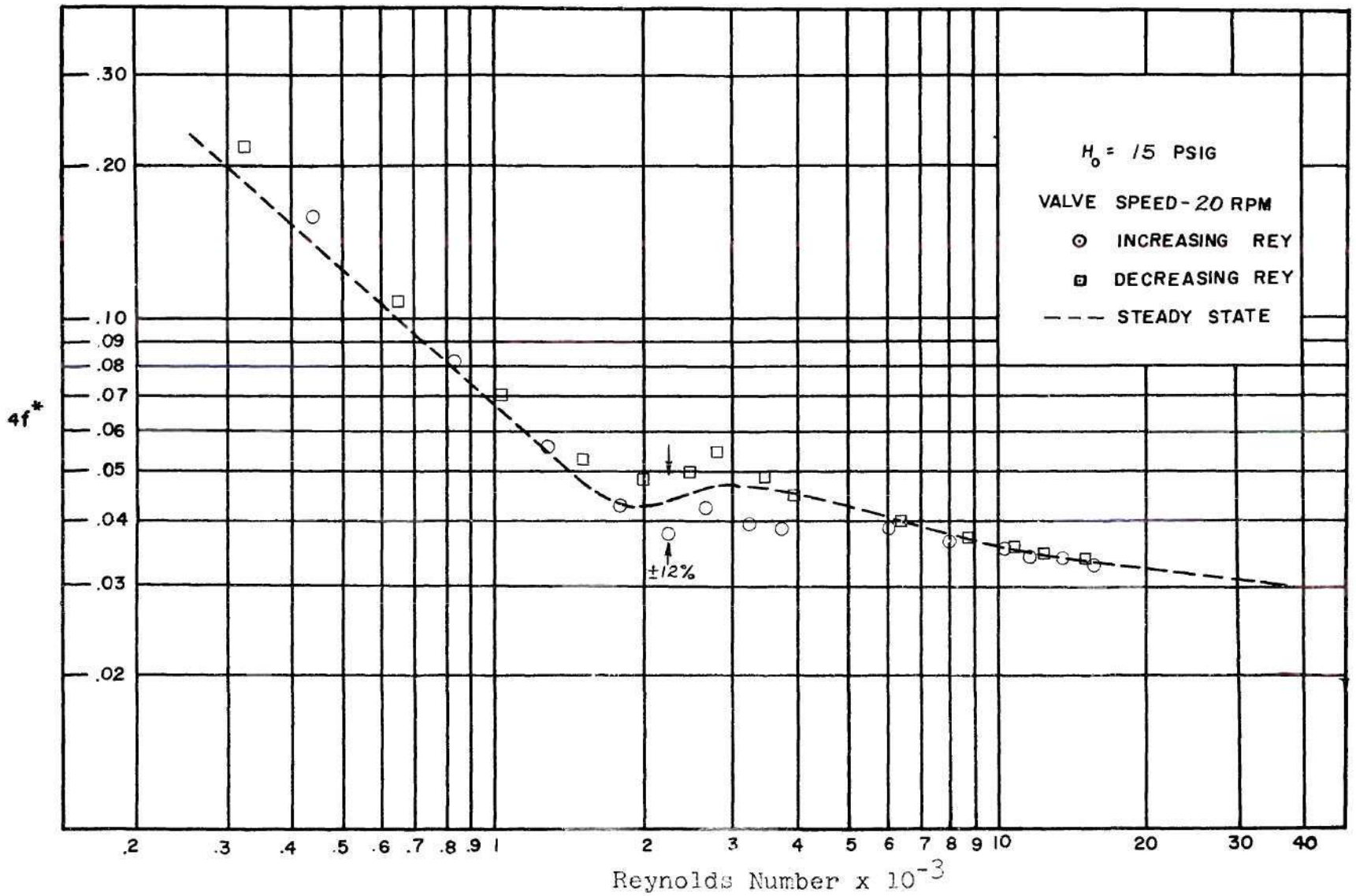

Fig. 15 Pseudo Friction Factor as a Function of Reynolds Number

CHAPTER V

CONCLUSIONS

The experimental results of this investigation will necessarily be limited to the single tube size, i.e., 0.290 inch I.D., and 145 inches long, with an L/D ratio of 500. Other limiting factors are the range of total head pressure used, of 10, 20, 40, 60 and 100 psig.

Also, the experimental results are limited to Reynolds numbers based on tube inside diameter varying from approximately 400 to 50,000.

With these restrictions, certain conclusions can be drawn from the experimental data:

1. The use of steady state methods in the determination of the pseudo friction factor gives accurate results for both laminar and turbulent unsteady flow.
2. The variation of pseudo friction factor with Reynolds number throughout the transition range has a definite form, and could possibly be correlated with total head pressure.
3. The time rate of change of Reynolds number on unsteady flow for both increasing and decreasing mass flow through the transition range has a very noticeable effect on the pseudo friction factor.

4. The value of pseudo friction factor for peak Reynolds number is not a function of time rate of change of mass flow or total head pressure.

CHAPTER VI

RECOMMENDATIONS

The author feels that the information derived from the present tests is not sufficient to draw general conclusions. Therefore, it is felt that certain expansions and refinements are necessary in order to obtain results which would be applicable to many particular cases.

The tests should be expanded for the purpose of including tubes of different lengths and other inside diameters. This expansion would encompass a wide range of length-to-diameter ratios, which would in turn give any effects of system geometry on the pseudo friction factors in unsteady flow. In particular, smaller diameter tubes should be tested in order to determine if the approach of choked flow has any noticeable effect on the pseudo friction factors correlation. However, this would necessarily reduce the maximum Reynolds numbers that might be obtained. Also, larger diameter tubes should be considered for the purpose of determining what, if any, rate effects could be detected, and how they affect the pseudo friction factors.

The present tests were all run at room temperatures, and as such, have a limited realm of applicability. Tests should be conducted with a controlled inlet temperature. These tests would indicate the effects of elevated temperatures

on the friction factors.

The manipulation of the isolation cut-off valves with each transducer proved to be quite troublesome at times. Since this operation is necessary for reasons pointed out in the presentation, a method should be utilized which would isolate these instruments at a predetermined pressure level. This not only would reduce the chances of exposing the transducers to a pressure level higher than which it is rated, but would also eliminate the human factor involved. Since the system itself is sensitive to manual vibrations, these would be eliminated also.

The effects of entrance reductions, in the form of union diameter to tube inside diameter ratios less than 1.0 should be considered also. This problem should be undertaken in order to indicate more substantially the validity of assuming steady state conditions. A correlation of data resulting from these tests with those of previous steady state tests by Lattal would further prove the steady state assumption.

APPENDIX A

The basic assumptions underlying the development of the equations for the pseudo friction factor are;

(1) One-dimensional

(2) Steady flow

(3) Continuum flow

(4) Constant area tubing

(5) Isothermal changes of state

The single assumption that seems unreasonable at this point is that of steady flow. Later it will be seen from the empirical curves that this assumption leads to reasonable results for the pseudo friction factor.

The development of the equations in the present section shall follow very closely that of Lattal.

For steady flow through a constant area tubing, with a control volume as shown in Figure 16, the continuity and

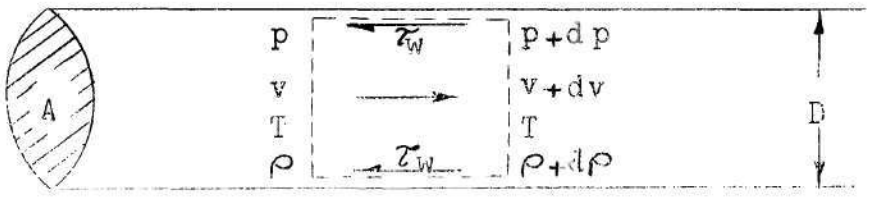

Figure 16. Control Volume Element

momentum equations may be written, respectively

$$\frac{w}{A} = \rho v = G, \text{ a constant} \qquad (A\text{-}1)$$

and

$$Adp + \tau_w \frac{4A}{D} dx + wdv = 0 \qquad (A-2)$$

where w is the rate of mass flow, A is the cross-sectional area of the tube, ρ is the density of the air, v is the mean velocity of the air across the section, p is the static pressure in the tube, τ_w is the shearing stress exerted on the stream by the walls, and $(4A/D)dx$ is the wetted area over which τ_w acts. Define the local friction factor as

$$f = \frac{\tau_w}{(1/2)\rho v^2} \qquad (A-3)$$

Introducing f into Equation (A-2), dividing by A, substituting for ρ from the perfect gas equation of state ($P=\rho RT$) and for ρV from the continuity equation gives

$$\frac{pdp}{RT} + \frac{1}{2}\left[\frac{W}{A}\right]^2 \cdot \frac{4fdx}{D} + \left[\frac{W}{A}\right]^2 \cdot \frac{dv}{v} = 0 \qquad (A-4)$$

Differentiating the continuity equation and substituting the result into Equation (A-4) yields

$$\frac{2pdp}{RT} + \left[\frac{W}{A}\right]^2 \left[\frac{4fdx}{D} - 2\frac{d\rho}{\rho}\right] = 0 \qquad (A-5)$$

Equation (A-5) is integrated between the pressures P_I and P_{II} and results in

$$\frac{P_I^2 - P_{II}^2}{RT} + \left[\frac{W}{A}\right]^2 \left[4f\frac{L}{D} - 2\ln\frac{\rho_{II}}{\rho_I}\right] = 0 \qquad (A-6)$$

where $\bar{f} = 1/L\int_{I}^{II} f\,dx$ is the mean friction factor within the tube, and L is $X_{II} - X_I$. It should be noted that $\bar{f}$ may contain development losses if X_I and X_{II} are taken at the tubing extremities. Now, $\rho_I/\rho_{II} = P_I/P_{II}$, and Equation (A-6) is solved for w as

$$w^2 = \frac{A^2}{RT} \cdot \frac{P_I^2 - P_{II}^2}{4\bar{f}\frac{L}{D} + 2\ln(P_I/P_{II})} \qquad (A\text{-}7)$$

Realizing that Equation (A-7) is applicable to fully-developed flow over the entire length of tubing with no entrance or exit losses included, a new friction factor, f^*, (called a pseudo friction factor) is defined that expresses the mass flow, w, as a function of P_1 and P_2 (static pressures upstream and downstream of test tube, respectively). The mass flow, w, is now shown to be

$$w^2 = \frac{A^2}{RT} \frac{P_1^2 - P_2^2}{4f^*(L/D)} \qquad (A\text{-}8)$$

where the pseudo friction factor, f^*, incorporates the compressibility effect $[2\ln(P_I/P_{II})]$, entrance and exit effects, and development effects. Equation (A-8) may now be solved explicitly for $4f^*$, yielding

$$4f^* = \frac{P_1^2 - P_2^2}{RT\frac{L}{D} \cdot \left[\frac{w}{A}\right]^2} \qquad (A\text{-}9)$$

The empirical results of this study will be determined by Equation (A-9).

APPENDIX B

DEVELOPMENT OF THE BASIC FLOW EQUATION THROUGH A SHARP-EDGED ORIFICE

Assuming that the flow is steady, incompressible, obeys the perfect gas law, and that there is no loss of energy from friction and no heat transfer between the fluid and the surrounding walls, the American Society of Mechanical Engineers developed the following equations for flow through a sharp-edged orifice.

Consider the stations 1 and 2 in Figure 17.

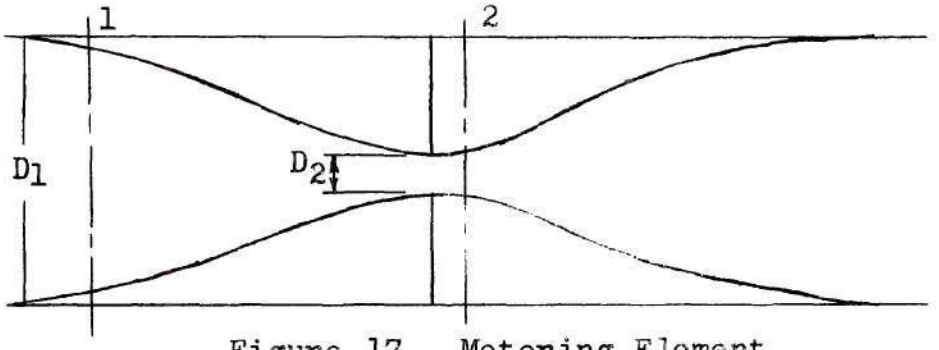

Figure 17. Metering Element

The well-known incompressible Bernoulli equation may be given as

$$(V_2^2 - V_1^2)\frac{\rho}{2g} = P_1 - P_2 = \Delta P \qquad \text{(B-1)}$$

where P_1, V_1, P_2, and V_2 are pressure and velocity at stations 1 and 2 respectively, ρ is the density, and g is the

acceleration due to gravity. The mass flow, w, is given by

$$w = \rho A_1 V_1 = \rho A_2 V_2 \qquad (B-2)$$

where A_1 and A_2 are the cross-sectional areas at stations 1 and 2, respectively.

The continuity equation (Equation (B-2)), may be solved as

$$V_1 = V_2 \left[\frac{D_2}{D_1}\right]^2 = V_2 B^2 \qquad (B-3)$$

where B is the ratio of orifice diameter to pipe diameter, D_2/D_1. Substituting (B-3) into (B-1) and simplifying gives

$$V_2 \frac{1}{\sqrt{1 - B^4}} \sqrt{\frac{2g\Delta P}{\rho}} \qquad (B-4)$$

Incorporating the continuity equation and equation of state ($P=\rho RT$) it may be shown that

$$w = \frac{A_2}{\sqrt{1 - B^4}} \cdot \sqrt{\frac{2gP_1\Delta P}{RT_1}} \qquad (B-5)$$

The ASME suggests the use of three empirical corrections (K, Y, E) to the above equation since the actual flow varies from the theoretical relations. The discharge coefficient, K, is a function of Reynolds number, the compressibility factor, Y, is a function of the B ratio and the pressure ratio, and E is a coefficient which corrects for the thermal expansion of the metering element.

For air the mass flow rate is given by

$$w = 1.10 \frac{A_2 KYE}{\sqrt{1 - B^4}} \sqrt{\frac{P_1 \Delta P}{T_1}} \qquad \text{(B-6)}$$

It should be noted that for the present study, with $B = 0.1$, the factor $\sqrt{1 - B^4}$ is essentially unity. Also, since isothermal flow is assumed, E is equal to unity. Now, using the equation of state, Equation (B-6) may be re-written as

$$w \quad 1.10 A_2 KY \sqrt{R \rho \Delta P} \qquad \text{(B-7)}$$

REFERENCES

1. Kármán, T. von, Mechanical Similitude and Turbulence, National Advisory Committee for Aeronautics, Technical Memorandum 611, 1931.

2. Nikuradse, J., Gesetzmassigkeiten der Turbulenten Stromung in Glatten Rohren, Forschungs-Arb. Ing.-Wesen, No. 356, 1932.

3. Schlichting, H., Boundary Layer Theory, Trans., Kestin, J., New York: McGraw-Hill Book Co., Inc., 1955, pp.400-406

4. Ibid, p. 63

5. Lattal, G. L., Correlation of Pressure Losses in Small Bore Tubing for Reynolds Numbers Between 400 and 50,000, Unpublished Master's Thesis, Georgia Institute of Technology, 1960.

6. Stone, G. W., Transient Response Characteristics of Simulated Missile Pneumatic Plumbing Systems Subjected to Shock Wave Inputs, Unpublished Master's Thesis, Georgia Institute of Technology, 1960.

7. Schultz-Grunow, F., Pulsierender Durchfluss durch Rohre, Forschungs-Arb. Ing.-Wesen, No. 11, 1940.

8. Fluid Meters, Their Theory and Application, Part I, The American Society of Mechanical Engineers, 1937.